International Journal of Heat and Mass Transfer 52 (2009) 5152–5157

Contents lists available at ScienceDirect

International Journal of Heat and Mass Transfer

journal homepage: www.elsevier.com/locate/ijhmt

# Effect of static magnetic field on a thermal conductivity measurement of a molten droplet using an electromagnetic levitation technique

Takao Tsukada [a,*], Ken-ichi Sugioka [a], Tomoya Tsutsumino [b], Hiroyuki Fukuyama [c], Hidekazu Kobatake [c]

[a] Department of Chemical Engineering, Tohoku University, 6-6-07, Aoba, Aramaki, Aoba-ku, Sendai 980-8579, Japan
[b] Department of Chemical Engineering, Osaka Prefecture University, 1-1 Gakuen-cho, Naka-ku, Sakai, Osaka 599-8531, Japan
[c] Institute of Multidisciplinary Research for Advanced Materials, Tohoku University, 2-1-1 Katahira, Aoba-ku, Sendai 980-8577, Japan

ARTICLE INFO

*Article history:*
Received 26 November 2008
Received in revised form 8 April 2009
Accepted 8 April 2009
Available online 13 June 2009

*Keywords:*
Static magnetic field
Electromagnetic levitation
Droplet
Molten silicon
Convection
Numerical simulation
Thermal conductivity

ABSTRACT

Recently, a novel method of measuring the thermophysical properties, particularly thermal conductivity, of high-temperature molten materials using the electromagnetic levitation technique has been developed by Kobatake et al. [H. Kobatake, H. Fukuyama, I. Minato, T. Tsukada, S. Awaji, Noncontact measurement of thermal conductivity of liquid silicon in a static magnetic field, Appl. Phys. Lett. 90 (2007) 094102]; this method is based on a periodic laser-heating method, and entails the superimposing of a static magnetic field to suppress convection in an electromagnetically levitated droplet. In this work, to confirm the fact that a static magnetic field really suppresses convection in a molten silicon droplet in an electromagnetic levitator, numerical simulations of convection in the droplet and periodic laser heating in the presence of convection have been carried out. Here, the convections driven by buoyancy force, thermocapillary force due to the temperature dependence of the surface tension on the melt surface, and electromagnetic force in the droplet were considered. As a result, it was found that applying a static magnetic field of 4 T can suppress convection in a molten silicon droplet enough to measure the real thermal conductivity of molten silicon.



## 1. Introduction

The electromagnetic levitation (EML) technique has become a widely used experimental technique for investigating solidification from an undercooled melt [1] and for measuring the thermophysical properties of molten materials [2]. In the EML technique, the alternating electric current in RF coils induces an eddy current in a conductive material sample, which is melted by joule heating from the current. In addition, the electromagnetic force caused by the interaction between an alternating magnetic field and the induced current lifts up the molten drop-shaped material. Such a containerless, EML technique allows melt to achieve deep undercooling for the formations of metastable phases and microstructures because it removes the risk of heterogeneous nucleation from the wall of the container. The EML technique also enables the precise measurement of the thermophysical properties of highly reactive molten materials over a wide temperature range even under an undercooled condition without contamination.

In the EML technique, it is well-known that the magnetohydrodynamic (MHD) convection due to electromagnetic force occurs in a molten droplet, together with buoyancy and Marangoni convections, and that the flow velocity reaches 10–40 cm/s [3–6]. Such melt convection may affect the thermal field and solidification in the droplet, and consequently the solidified structure and measured thermophysical properties. Recently, Yasuda et al. [7] have investigated the effect of convection in an electromagnetically levitated droplet on the microstructures of metallic alloys, where a static magnetic field was superimposed to suppress and control melt convection. They demonstrated experimentally that the reduction in melt flow causes microstructural transition in solidified alloys. Kobatake et al. [8,9] measured the thermal conductivity of molten silicon, using an electromagnetic levitator installed inside a superconducting magnet and based on the periodic laser-heating method. The static magnetic field allowed them to precisely measure thermal conductivity, because it removes the contribution of convective heat transfer to the measured values. The magnetic field suppression of the melt flow has been used in various industrial areas, particularly in the single crystal growth of semiconductors for the production of high-quality crystals, and many numerical studies have been carried out to gain physical insights into the flow and thermal fields in the melt under a magnetic field [10,11]. However, there were few studies on the effect of the magnetic field suppression on convection in an electromagnetically levitated droplet [5].

In this work, we numerically investigated the effect of a static magnetic field on melt convection in a silicon droplet levitated in an electromagnetically levitator used by Kobatake et al. to measure

* Corresponding author. Tel./fax: +81 22 795 7260.
*E-mail address:* tsukada@pcel.che.tohoku.ac.jp (T. Tsukada).

0017-9310/$ - see front matter © 2009 Elsevier Ltd. All rights reserved.
doi:10.1016/j.ijheatmasstransfer.2009.04.020

**Nomenclature**

| | |
|---|---|
| $A$ | angular component of magnetic vector potential [Wb/m$^3$] |
| $B_0$ | magnetic flux density [T] |
| $C_p$ | specific heat [J/kg K] |
| $\boldsymbol{e}_r$ | unit vector in $r$-direction [–] |
| $\boldsymbol{e}_\phi$ | unit vector in azimuthal direction [–] |
| $\boldsymbol{e}_\theta$ | unit vector in $\theta$-direction [–] |
| $g$ | gravitational acceleration [m/s$^2$] |
| $J$ | electric current density [A/m$^2$] |
| $J_0$ | electric current density in RF coil [A/m$^2$] |
| $j$ | $=\sqrt{-1}$ |
| $k$ | thermal conductivity [W/m K] |
| $\boldsymbol{n}$ | unit normal vector |
| $p$ | pressure [Pa] |
| $P$ | laser power [W] |
| $R$ | droplet radius [m] |
| $r$ | radial distance in spherical coordinates [m] |
| $T$ | temperature [K] |
| $T_a$ | ambient temperature [K] |
| $T_m$ | melting point temperature [K] |
| $t$ | time [s] |
| $\boldsymbol{t}$ | unit tangential vector |
| $\boldsymbol{u}$ | velocity vector [m/s] |
| $u_r$ | $r$-component of velocity vector [m/s] |
| $u_\theta$ | $\theta$-component of velocity vector [m/s] |
| $\varepsilon$ | emissivity [–] |
| $\phi$ | stream function [m$^3$/s] |
| $\Delta\phi_s$ | phase lag [°] |
| $\gamma$ | surface tension [N/m] |
| $\mu_0$ | magnetic permeability [H/m] |
| $\mu$ | viscosity [Pa s] |
| $\nu$ | kinematic viscosity [m$^2$/s] |
| $\theta$ | polar angle in spherical coordinates [rad] |
| $\rho$ | density [kg/m$^3$] |
| $\sigma$ | electrical conductivity [S/m] |
| $\sigma_{SB}$ | Stefan–Boltzmann constant [W/m$^2$ K$^4$] |
| $\boldsymbol{\tau}$ | stress tensor [Pa] |
| $\omega$ | frequency of modulated light source [rad] |
| $\omega_{RF}$ | frequency of current in the RF coil [rad/s] |

*subscript*

| | |
|---|---|
| $a$ | free space |
| $c$ | RF coil |
| $m$ | molten silicon |
| $max$ | maximum |
| $min$ | minimum |

*superscript*

| | |
|---|---|
| $*$ | conjugate complex |

the thermal conductivity [8,9]. Kobatake et al. revealed that the measured values are insensitive to magnetic field strength above 2 T, and considered that the commonly used strength of 4 T is sufficient to precisely measure the thermal conductivity of molten silicon, although no melt convection is observed experimentally. The primary aim of this work is to numerically confirm the following issues: (1) How much is the velocity field in the droplet dumped by applying a static magnetic field? (2) How much does the measured thermal conductivity vary by applying a static magnetic field?

## 2. Model formulations and methodology

### 2.1. Electromagnetic, flow and temperature fields in a molten droplet

Fig. 1 shows a schematic diagram of the EML system used to measure the thermal conductivity of molten silicon [8,9]. Here, the MHD convection and additionally the buoyancy and Marangoni convection in the droplet are suppressed by applying an axial static magnetic field $B_0$. In the numerical simulation of the EML system, the electromagnetic field in the system should first be computed to obtain electromagnetic force and the distribution of heat generation rate in the droplet, and then the flow and temperature fields in the droplet are calculated.

In the numerical simulation of electromagnetic field, the following were assumed: (1) the shape of the droplet is spherical, (2) the system is axially symmetric, (3) the media are linear, isotropic and stationary, (4) the displacement current is unimportant in this situation and (5) there is no net charge in the system. Under these assumptions, Maxwell's equation can be transformed into the following equation in spherical coordinates:

$$\nabla^2 A_i - \frac{A_i}{r^2 \sin^2\theta} = -\mu_0 J_i \quad (i = m, c \text{ or } a), \tag{1}$$

where molten silicon, the RF coil and free space are denoted '$m$', '$c$' and '$a$', respectively. $J_i$ and $A_i$ are the angular components of the current density and the vector potential, respectively. Because every physical quantity can be assumed to have a conventional harmonic time dependence, $\exp(j\omega_{RF}t)$, $A_i$ in Eq. (1) is replaced with the complex variable $\dot{A}_i$, and $J_i$ is given by $-j\sigma\omega_{RF}\dot{A}_i$ in the droplet, by $J_0$ in the RF coil and by zero in free space. The boundary conditions at the centerline and infinity for $\dot{A}_i$ are

$$\dot{A}_i = 0. \tag{2}$$

The flow and temperature distributions in a molten silicon droplet are expressed by (3)–(5), i.e., the continuity, Navier–Stokes and energy equations, under the following assumptions: (1) the droplet shape is spherical, (2) the system is axially symmetric, (3) the flow is laminar and the fluid is incompressible, and (4)

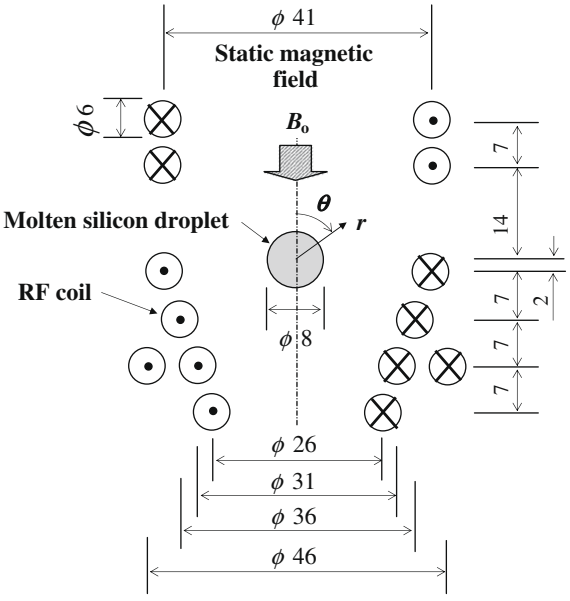


**Fig. 1.** Schematic diagram of electromagnetic levitator with a static magnetic field.

the thermophysical properties of the melt are constant except for the temperature dependences of density and surface tension, in the calculations of the buoyancy force and the Marangoni effect, respectively.

$$\nabla \cdot \boldsymbol{u} = 0, \tag{3}$$

$$\rho\left[\frac{\partial \boldsymbol{u}}{\partial t} + \nabla \cdot (\boldsymbol{u}\boldsymbol{u})\right] = -\nabla p + \mu \nabla \cdot (\nabla \boldsymbol{u} + \nabla \boldsymbol{u}^T) + \frac{1}{2}\sigma\omega_{RF}\mathrm{Re}\left[j\left(\dot{A}^* \boldsymbol{e}_\phi\right) \times \nabla \times \left(\dot{A}\boldsymbol{e}_\phi\right)\right] - \sigma B_0^2 (u_r \sin\theta + u_\theta \cos\theta) \times (\sin\theta \boldsymbol{e}_r + \cos\theta \boldsymbol{e}_\theta) - \rho g(\cos\theta \boldsymbol{e}_r - \sin\theta \boldsymbol{e}_\theta), \tag{4}$$

$$\rho C_p\left[\frac{\partial T}{\partial t} + \nabla \cdot (\boldsymbol{u}T)\right] = k\nabla^2 T + \frac{1}{2}\sigma\omega_{RF}^2(\dot{A}^*\dot{A}), \tag{5}$$

where Re[ ] in Eq. (4) indicates the real part of complex quantity.

The boundary conditions for (3)–(5) are given by the following equations.

At the droplet surface:

$$\tau : \boldsymbol{n}\boldsymbol{t} = \left(-\frac{\partial \gamma}{\partial T}\right)\nabla T \cdot \boldsymbol{t}, \quad \boldsymbol{u} \cdot \boldsymbol{n} = 0 \tag{6, 7}$$

$$-k\nabla T \cdot \boldsymbol{n} = \varepsilon\sigma_{SB}\left(T^4 - T_a^4\right) \tag{8}$$

At the centerline:

$$\tau : \boldsymbol{n}\boldsymbol{t} = \boldsymbol{n} \cdot \boldsymbol{u} = \nabla T \cdot \boldsymbol{n} = 0 \tag{9-11}$$

As shown in Fig. 1, this system is in unbounded free space. Thus, a particular means is necessary to solve the electromagnetic field. In this study, the hybrid finite difference method (FDM) and boundary element method (BEM) were used [12], where the mathematical domain I to be solved by the FDM is the droplet and part of the free space around the droplet, while the domain II to be solved by the BEM is the free space around domain I including the RF coil. For the discretization of the BEM, constant elements were used, where the potential and its flux were assumed to be constant over each element at the boundary of domain II. On the other hand, Eq. (1) in domain I was discretized by a second-order central differential scheme.

The governing equations for flow and temperature fields were solved numerically by employing the control-volume-based, finite difference technique, and the SIMPLER algorithm [13] is used to obtain the velocity field by coupling the continuity and momentum equations.

The number of grids in the droplet was 80 (in $r$-direction) $*$ 100 (in $\theta$-direction), and the number of grids in the free space was 30 (in $r$-direction) $*$ 100 (in $\theta$-direction) in both the analyses of electromagnetic field and velocity and temperature fields. The grids were arranged such that dense grids were applied near the droplet surface.

### 2.2. Determination of thermal conductivity of a droplet

For the measurement of the thermal conductivity of a molten silicon droplet, Kobatake et al. [8,9] adopted the periodic laser-heating method [14,15]. In this method, the upper part of an electromagnetically levitated droplet was periodically heated by a modulated laser light source, and the temperature variation at the lower part of the droplet caused by heat flow from the upper part through the droplet was detected by a pyrometer. Then, the phase lag between the modulated light and the temperature variations detected by the pyrometer, $\Delta\phi_s$, was measured at various frequencies of the modulated light, $\omega$. The relation between $\Delta\phi_s$ and $\omega$ obtained experimentally was fitted by the mathematical model to estimate the thermal conductivity, where the unsteady-state heat conduction equation for the droplet accompanying radiative heat transfer to the ambient was simplified and transformed to steady-state linear equations [14]. In this work, the relation between $\Delta\phi_s$ and $\omega$ is obtained numerically. The temperature responses at the lower part of the droplet are evaluated by solving the thermal advection–conduction equation for the droplet when the upper part is periodically heated by a modulated laser light source, where the flow field in the droplet described in the previous section is fixed assuming that the flow field is not affected by periodic heating. This assumption is made for the following reasons, although, strictly peaking, it might not be correct: (1) the time step needed in the calculation of melt convection is too small compared with the period of laser heating and (2) the predominant flow in the droplet is the MHD convection.

## 3. Results and discussion

Before numerically investigating the effect of the application of a static magnetic field on convection in a molten silicon droplet, it is important to ascertain the reliability and accuracy of the present simulation. First, the results of the simulations of the electromagnetic field that controls MHD convection and heat transfer in the droplet were compared with the analytical and experimental data of power absorption and lifting force for the positioning coils of TEMPUS as Zong et al. have carried out [3]. Fig. 2 shows a comparison of the measured lifting forces and the analytical results of power absorption with the present calculation results as a function of the position of the sample along the central axis. It is found that the present results are in good agreement with the experimental and analytical ones.

For the numerical simulations of convection in an electromagnetically levitated droplet including MHD convection, the numerical results obtained by Li and Song [4] were compared with our results, where Marangoni and MHD convections in a 10-mm diameter silver droplet, electromagnetically levitated by a positioning coil of the TEMPUS facility in a microgravity environment were calculated numerically. Fig. 3 shows the velocity vectors and isotherms in the droplet calculated in this work. There are four vortices induced by the electromagnetic force in the droplet, which were also observed in ref. [4]. Comparing the maximum velocity in the droplet in this work with that in ref. [4], the former is 5.35 cm/s and the latter is 4.39 cm/s. Although there is some discrepancy between them, it seems that our numerical simulation is relatively reasonable, considering that Li and Song [4] used the finite element method as a numerical procedure and specified no details of their discretizations, and that the absolute value of the velocity in the MHD convection strongly depends on discretized mesh size.

Table 1 shows the physical properties of the molten silicon and the operating conditions of the electromagnetic levitator used in

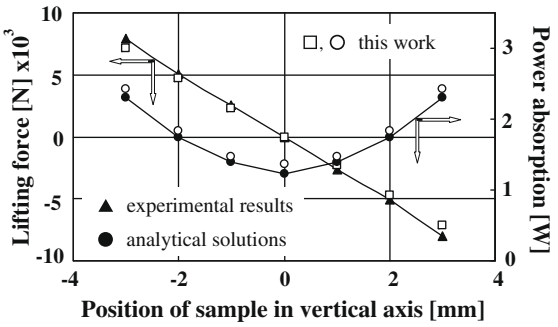


**Fig. 2.** Comparison of numerical, analytical and experimental results for lifting force and power absorption in TEMPUS devise for a 10-mm diameter copper sphere.

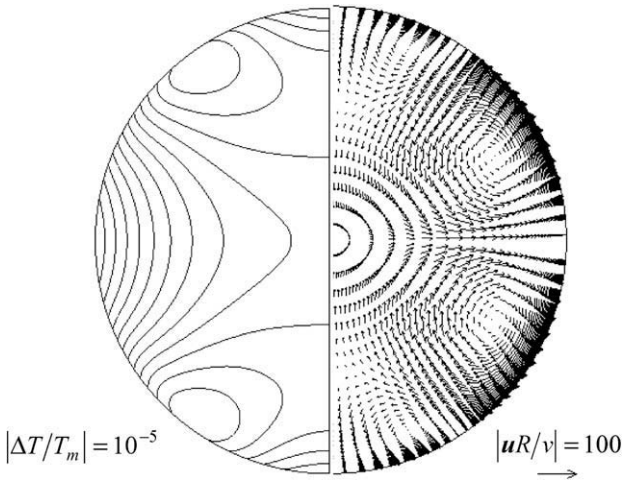


**Fig. 3.** Convection in a silver droplet with a diameter of 10 mm, electromagnetically levitated by a positioning coil of TEMPUS devise under microgravity environment.

**Table 1**
Physical properties and processing conditions used in calculations.

| | |
|---|---|
| *Physical properties of molten silicon* | |
| Temperature coefficient of surface tension [N/(m K)] | $-4.3 \times 10^{-4}$ |
| Viscosity [Pa s] | $7.0 \times 10^{-4}$ |
| Density [kg/m$^3$] | 2530 |
| Thermal expansion coefficient [1/K] | $1.5 \times 10^{-4}$ |
| Thermal conductivity [W/(m K)] | 64.0 |
| Emissivity [–] | 0.3 |
| Specific heat [J/(kg K)] | 1000 |
| Electric conductivity [S/m] | $1.2 \times 10^6$ |
| Melting temperature [K] | 1683 |
| *Operating conditions* | |
| Electric current in RF coil [A] | 402.2 |
| Frequency of electric current in RF coil [kHz] | 200 |
| Magnetic flux density [T] | 1–5 |
| Ambient temperature [K] | 323 |

this work, where the operating conditions were the same as those used in the measurement of thermophysical properties [8,9]. The geometry of the RF coils is the same as that in Fig. 1 and the diameter of the molten silicon droplet is $8 \times 10^{-3}$ m. The electric current in the RF coil, 402.2 A, is the value which is necessary to levitate the molten silicon droplet at the position shown in Fig. 1. Here, the levitation of the droplet is based on the balance between the electromagnetic force and gravity force acting on the droplet. In the actual experiments, the electric current in the RF coil is varied depending on the measuring temperature, and consequently, the droplet position also changes.

Fig. 4 shows the velocity profiles, stream lines and isotherms in the molten silicon droplet without the laser heating, where a static magnetic field of 4 T is axially applied. In this case, the solutions reached the steady-state ones. In this work, the convections induced by buoyancy force, thermocapillary force due to the temperature dependence of the surface tension on the melt surface, and electromagnetic force in the droplet were considered. Among them, the MHD convection induced by electromagnetic force has a very high velocity, e.g., more than 10 cm/s; moreover, fluid flow in the droplet is within the mild turbulent flow regime [3–6]. Therefore, some previous studies used the $k-\varepsilon$ turbulent model [3] or increased viscosity [4] to account for the turbulent behavior in the electromagnetically levitated droplet. In contrast, because we assumed a laminar melt flow to consider convection under a static magnetic field, we cannot calculate convection without the static magnetic field. From the figures, it can be seen that convection in the droplet is markedly suppressed by an applied static magnetic field. A static magnetic field can suppress the flow perpendicular to the direction of the magnetic field, i.e., the radial flow in the droplet, but cannot suppress the axial component of the flow. As a result, three longitudinal vortices appear in the droplet. Particularly, relatively intense flows, namely, the Marangoni and MHD convections, remain near the surface of the equatorial part of the droplet. However, because the maximum velocity $|\boldsymbol{u}_{max}R/\nu|$ is 614.15, i.e., 4.25 cm/s in dimensional velocity, which must be much less than that without the magnetic field, and the velocity of the fluid flow near the centerline is less than 1 cm/s, convection in the droplet can be apparently suppressed. Here, the velocity along the droplet surface, i.e., $u_\theta$ at $r = R$, is not considered when the maximum velocity is evaluated.

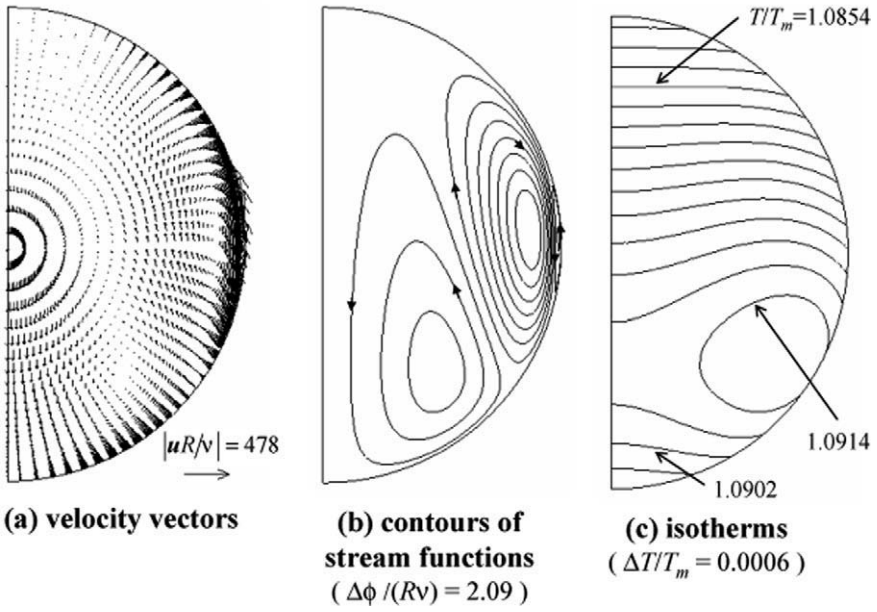


**Fig. 4.** Effect of a static magnetic field on the velocity and temperature fields in an electromagnetically levitated molten silicon droplet, where the magnetic flux density $B_0$ is 4 T.

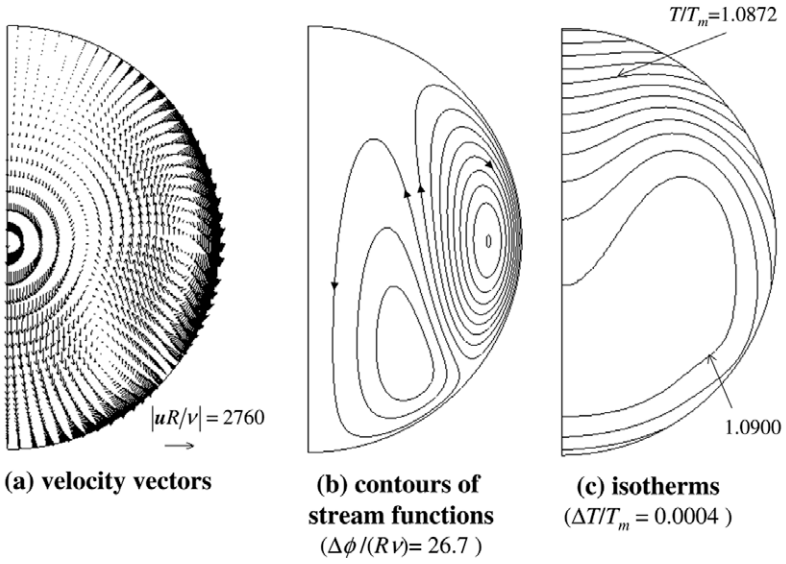


**Fig. 5.** Effect of a static magnetic field on the velocity and temperature fields in an electromagnetically levitated molten silicon droplet, where the magnetic flux density $B_0$ is 1 T.

Fig. 5 shows the results for 1 T without the laser heating. In this case, the solutions also reached the steady-state ones. From the figures, it can be seen that convection in the droplet becomes markedly intense as applied static magnetic field decreases. Particularly, the MHD convection is dominant, and consequently the counterclockwise vortex due to the Marangoni convection near the surface of the equatorial part of the droplet disappears, although the Marangoni convection can be observed for 4 T in Fig. 4. The maximum velocity $|\boldsymbol{u}_{max}R/\nu|$ in the droplet is 3095.2, i.e., 21.4 cm/s in dimensional velocity, and the velocity of the fluid flow near the centerline is approximately 10.8 cm/s.

In addition, comparing between the temperature distributions inside the droplet for 4 and 1 T (see Figs. 4 and 5(c)), it can be seen that the temperature field is strongly affected by convection when the applied magnetic field is relatively small. Since the Prandtl number of silicon melt, approximately $10^{-2}$, is small, conduction heat transfer becomes relatively dominant compared to convection in the melt. Consequently, the temperature field for 4 T is insusceptible to the melt flow. However, for 1 T, the intensive convection deforms the isotherms in the droplet, even though the Prandtl number is relatively small.

Next, the effect of a static magnetic field, i.e., convection in a molten silicon droplet, on thermal conductivity is investigated numerically by calculating the temperature fields in the droplet during periodic laser heating. Here, it is considered that the flow fields in the droplet are not affected by periodic laser heating, and thus the thermal advection–conduction equation is solved under a given flow field as shown in Figs. 4 or 5(a). Fig. 6 shows the calculated temperature response at the lower part of the droplet surface when the upper part of the droplet is irradiated with a modulated laser beam with a frequency of 0.1 Hz and a power amplitude of 9.56 W, while applying a static magnetic field of 4 T. Here, the distribution of laser intensity is assumed to be Gaussian, and the $e^{-2}$ radius of the laser beam is 2.0 mm. The temperature, which is the integral mean over the region corresponding to the pyrometer spot radius of 2.0 mm, exhibits increases in average temperature and modulation amplitude from the initial temperature, and ultimately reaches the stationary modulation state with certain constant average temperature and amplitude.

Calculations similar to those in Fig. 6 were carried out by varying the frequency of the modulated laser beam, $\omega$, and static magnetic field. The plots in Fig. 7 show the relation between the phase lag $\Delta\phi_s$ and $\omega$ calculated numerically for three different static magnetic fields, where $\Delta\phi_s$ is the phase lag between the modulated laser beam and the temperature variations at the lower part of the droplet surface. Then, the mathematical model proposed in our previous work [14] is adopted to obtain thermal conductivity from the plots in Fig. 7, as shown by a fitting line in the figure. Consequently, thermal conductivity is obtained for each static magnetic field. Fig. 8 shows the effect of static magnetic field on thermal conductivity obtained from the relation between $\Delta\phi_s$ and $\omega$ shown in Fig. 7, where thermal conductivity is normalized by its value at

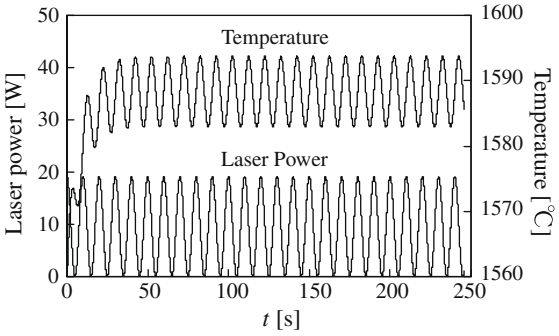


**Fig. 6.** Calculated temperature respond at the lower part of the droplet when the upper part is irradiated by the modulated laser beam.

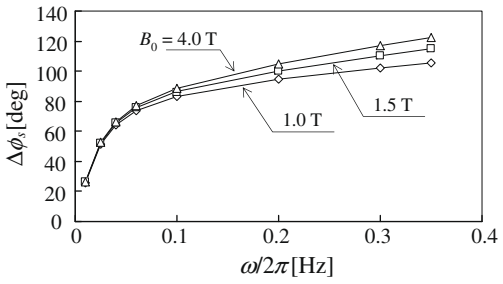


**Fig. 7.** Calculated relation between phase lag $\Delta\phi_s$ and frequency $\omega$ for the three different static magnetic fields.

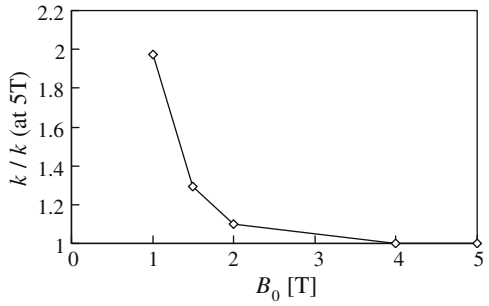


**Fig. 8.** Effect of the static magnetic field on thermal conductivity.

5 T, i.e., 64.9 W/m K. Comparing the thermal conductivity evaluated at 5 T with the input data in Table 1, both values show good agreement, and consequently, it can be seen that the thermal conductivity at 5 T is not affected by convection in the droplet. From the figure, thermal conductivity increases suddenly, namely, it is strongly affected by convection in the droplet when the static magnetic field becomes less than 2 T; thus, it can be concluded that the magnetic field should be more than at least 4 T for the measurement of the thermal conductivity of molten silicon by the EML technique.

## 4. Conclusions

To confirm the fact that a static magnetic field really suppresses convection in a molten silicon droplet in an electromagnetic levitator, which was used to measure the thermophysical properties of molten silicon, numerical simulations of convection in the droplet and periodic laser heating in the presence of convection have been carried out. Here, the convections driven by buoyancy force, thermocapillary force due to the temperature dependence of the surface tension on the melt surface, and electromagnetic force in the droplet were considered. As a result, applying a static magnetic field of 4 T can suppress convection in the droplet enough to measure the real thermal conductivity of molten silicon.

## Acknowledgement

This development was supported by SENTAN, JST.

## References

[1] D. Herlach, R. Cochrane, I. Egry, H. Fecht, L. Greer, Containerless processing in the study of metallic melts and their solidification, Int. Mater. Rev. 38 (1993) 273–373.
[2] I. Egry, A. Diefenbach, W. Dreier, J. Piller, Containerless processing in space – thermophysical property measurements using electromagnetic levitation, Int. J. Thermophys. 22 (2001) 569–578.
[3] J.H. Zong, B. Li, J. Szekely, The electromagnetic and hydrodynamic phenomena in magnetically-levitated molten droplets – I. Steady state behavior, Acta Astronaut. 26 (1992) 435–449.
[4] B.Q. Li, S.P. Song, Thermal and fluid flow aspects of electromagnetic and electrostatic levitation – a comparative modeling study, Microgravity Sci. Technol. XI (1998) 134–143.
[5] V. Bojarevics, K. Pericleous, Modeling electromagnetically levitated liquid droplet, ISIJ Int. 43 (2003) 890–898.
[6] R.W. Hyers, Fluid flow effects in levitated droplets, Meas. Sci. Technol. 16 (2005) 394–401.
[7] H. Yasuda, I. Ohnaka, R. Ihshii, S. Fujita, Y. Tamura, Investigation of the melt flow on solidified structure by a levitation technique using alternative and static magnetic fields, ISIJ Int. 45 (2005) 991–996.
[8] H. Kobatake, H. Fukuyama, I. Minato, T. Tsukada, S. Awaji, Noncontact measurement of thermal conductivity of liquid silicon in a static magnetic field, Appl. Phys. Lett. 90 (2007) 094102.
[9] H. Kobatake, H. Fukuyama, I. Minato, T. Tsukada, S. Awaji, Noncontact modulated laser calorimetry of liquid silicon in a static magnetic field, J. Appl. Phys. 104 (2008) 054901.
[10] D. Vizman, S. Eichler, J. Friedrich, G. Muller, Three-dimensional modeling of melt flow and interface shape in the industrial liquid-encapsulated Czochralski growth of GaAs, J. Crystal Growth 266 (2004) 396–403.
[11] L.J. Liu, K. Kakimoto, Partly three-dimensional global modeling of a silicon Czochralski furnace. II. Model application: analysis of a silicon Czochralski furnace in a transverse magnetic field, Int. J. Heat Mass Transfer 48 (2005) 4492–4497.
[12] A.F. Kolesnichenko, A.D. Podoltsev, I.N. Kucheryabaya, Action of pulse magnetic field on molten metal, ISIJ Int. 34 (1994) 715–721.
[13] S.V. Patanker, Numerical Heat Transfer and Fluid Flow, Hemisphere, New York, 1980, pp. 113–137.
[14] T. Tsukada, H. Fukuyama, H. Kobatake, Determination of thermal conductivity and emissivity of electromagnetically levitated high-temperature droplet based on the periodic laser-heating method: theory, Int. J. Heat Mass Transfer 50 (2007) 3054–3061.
[15] H. Fukuyama, H. Kobatake, K. Takahashi, I. Minato, T. Tsukada, S. Awaji, Development of modulated laser calorimetry using a solid platinum sphere as a reference, Meas. Sci. Technol. 18 (2007) 2059–2066.